Modeling and Dynamics of a Fuel Cell Combined Heat Power System for Marine Applications

VASILIS TSOURAPAS   JING SUN   ANNA STEFANOPOULOU*

Department of Naval Architecture and Marine Engineering

University Of Michigan

NAME Bldg, 2600 Draper Rd. Ann Arbor, MI 48109-2145

USA

djvas@umich.edu   http://www.engin.umich.edu/dept/name/name.html

Abstract: A control-oriented dynamic model of a fuel processor with a catalytic burner (CB) is developed using physics-based principles and is integrated with a proton exchange membrane fuel cell (PEM-FC) stack model. The fuel processor converts a hydrocarbon fuel to a hydrogen rich mixture that can be directly fed to the PEM-FC stack. Physics based component models are explored to gain fundamental understandings of system and subsystem level interactions. Our model captures the temporal evolution of gas pressures, gas compositions and reactor temperatures needed to describe H_2 generation and utilization. The low order model sheds light to critical transient conditions such as, H_2 starvation during load (current) transients. The model will serve as a critical enabling tool for future control system development.

Key-Words: Marine, Fuel Cell, Partial Oxidation, Catalytic Burner, Combined Heat Power System

1   Introduction

The feasibility of fuel cell systems for marine applications, especially for marine propulsion, is a topic still under research. The availability and accessibility of fueling resources, among other things, is a basic consideration in determining whether onboard fuel cell systems will become a viable alternative propulsion power for future ships. Inadequate infrastructure for hydrogen distribution and storage limits the applications of those fuel cells fueled by hydrogen. This limitation makes the fuel processor technology an important integral part of future marine fuel cell systems.

Efficient electric power distribution, flexible hull design, silent operation and low thermal acoustic signature are just some of the benefits made possible by integrating fuel cell and fuel processor system onboard military or commercial vessels. Furthermore, the capability to support large electric loads, with high efficiency even at low operating points, makes them suitable for supplying auxiliary power for service operation in passenger or cruise marine vessels.

The combined fuel cell and fuel processor system modeled in this paper has a rated power of 250KW, and uses natural gas as a fuel. Although the desired rated power and fuel for military or passenger ships differ from those of this model, the challenges presented here, are ubiquitous to all fuel cell power systems. In particular, albeit the target fuel for the navy is JP-8 and for the commercial vessels is crude oil, fast

H_2 generation and accurate temperature control of all the fuel processor reactors are generic and appear in the natural gas fueled system as well. The reforming of the complex and heavy hydrocarbons in the JP-8 or in crude oil is a daunting task which will of course pose even more challenges than the natural gas reforming.

With advanced fuel processing system technology, natural gas, which is widely available with extended distribution systems [1], can be reformed on-board ships. Common methods of converting natural gas to hydrogen include steam reforming and partial oxidation. An integrated partial oxidation based fuel processor and a fuel cell system has been investigated in [2], where a dynamic system model was developed and validated. For the system considered in [2], the central reactor of the fuel processing system (FPS) is a catalytic partial oxidation (CPOX) reactor. Hydrogen-rich gas is produced by mixing natural gas with air over a catalyst bed. The amount of hydrogen in the FPS depends on both the catalyst bed temperature and the CPOX air to fuel ratio, more specifically, the oxygen to carbon ratio. The CPOX bed temperature depends on the inlet gas temperature and the heat generated by the reaction at the oxygen to carbon ratio achieved before the reactor. To promote the reactions inside the CPOX unit, the air and fuel need to be pre-heated before entering the FPS. Possible FPS configurations used today are shown in Fig. 1.

In this paper, we investigate the fuel cell and fuel processor system that incorporates a catalytic burner (CB) to preheat the FPS inlet flow, by burning the excess H_2 that is not utilized in the fuel cell stack. The

---

*University of Michigan, Ann Arbor, MI
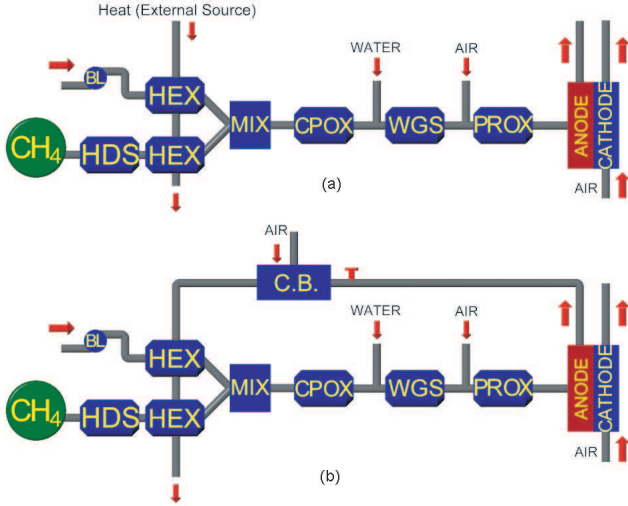Department of Mechanical Engineering

Fig. 1: FPS components with (a) and without (b) a Catalytic Burner

system diagram is shown in Fig. 1(b). A low order, 16 states, control-oriented model was implemented in Matlab SIMULINK. The model captures the dynamics coupled with the catalytic burner recirculation loop and is suitable for dynamics analysis, model-based control design and control system performance evaluation. Our analysis shows that this combined heat power (CHP) system provides higher overall efficiency as anticipated, while a substantial challenge appears in controlling its transient response during large load changes.

2   Problem Formulation

The transient response and the overall performance of the integrated systems shown in Fig. 1 is strongly coupled to the H_2 utilization in the anode, defined as the ratio of H_2 mass flow reacted in the anode to the mass flow supplied. In anticipation of possible load changes, the ideal 100% H_2 utilization is neither possible nor desirable. Hydrogen starvation, which takes place when the partial pressure of H_2 in the anode is zero, could damage the anode. Under typical operating conditions, the anode utilizes around 80% of the H_2 provided by the FPS [3]. As a result, the flow exiting the anode is still rich in energy content. Leaving the excess H_2 in the fuel cell exhaust not only compromises the efficiency, but also may cause other environmental and safety concerns.

A catalytic burner introduced in Fig. 1(b), can be used to recuperate the energy loss associated with the excess H_2 in the anode exhaust and convert it to thermal energy. This energy can be used to pre-heat the air and the natural-gas before entering the fuel processor, thus reduce the dependence on an external heat source for pre-heating. The conversion efficiency of the fuel processor, without taking into account the energy consumed by the auxiliary equipment, is given by

$$\eta_{with\ CB}^{FPS} = \frac{W_{produced}^{H_2} \cdot Q_{LHV}^{H_2}}{W_{used}^{CH_4} \cdot Q_{LHV}^{CH_4}} \tag{1}$$

$$\eta_{without\ CB}^{FPS} = \frac{W_{produced}^{H_2} \cdot Q_{LHV}^{H_2}}{(W_{used}^{CH_4} \cdot Q_{LHV}^{CH_4} + Q_{preheat})} \tag{2}$$

where $Q_{LHV}^{H_2}$ and $Q_{LHV}^{CH_4}$ are the lower heating values of hydrogen and methane, respectively, and $Q_{preheat}$ is the energy spent to preheat the inlet FPS flow. Fig. 2 compares the system efficiency for the two configurations shown in Fig. 1. It shows that up to 20% efficiency improvement can be obtained by the CHP system by recuperating the heat through a catalytic burner. The curve shown in the middle dashed line represents the efficiency of the CHP system using a feedforward control configuration. By using more elaborate control schemes, like feedback control, will allow us to maximize the overall FPS efficiency and reach levels shown in the upper dotted line.
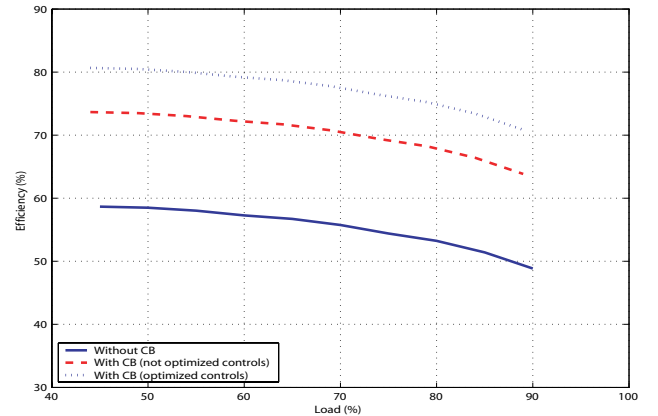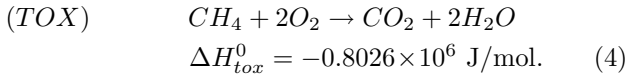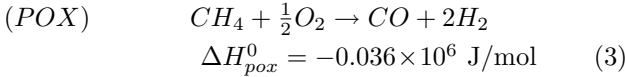

Fig. 2: Fuel Processor Efficiency Map

While the steady-state benefits of introducing the catalytic burner are rather obvious and overwhelming, transient problems when using the CHP system arise during large load changes. For example, when a large load is applied and the power demand suddenly increases, the H_2 utilization in the anode also increases. This could starve the CB of H_2, leading to a reduced temperature in the preheater. If the temperature falls below a certain threshold, the H_2 production in the CPOX will be demoted, resulting in poor H_2 generation, and in more severe situations, fuel cell damage. Another scenario is during a load decrease, when the anode H_2 utilization suddenly drops due to a decrease in the load demand. In this case, too much H_2 could flood the CB, leading to excessive heat that could cause overheating and destroy the burner.

To address the control and dynamics issues associated with the CHP system, a low-order model of the overall system is created to analyze the performance and facilitate the model-based control optimization.

3   Overview of the CHP System

The FPS is composed of four main reactors, namely, hydro-desulfurizer (HDS), catalytic partial oxidation (CPOX), water gas shift (WGS), and preferential oxidation (PROX). Natural gas, rich in methane CH_4, is supplied to the FPS from a tank. All FPS and FC

components operate at low pressures. An HDS is required for removing the sulfur from the natural gas [1, 4]. Sulfur is typically present in all natural gas distribution grids and degrades the catalysts in WGS and FC [5]. The main air flow is supplied to the system by a blower (BL) which draws air from the atmosphere. The air and the fuel are then pre-heated in separate heat exchangers (HEX). The heated air and the heated de-sulfurized natural gas stream are then mixed in the mixer (MIX). The mixture is then passed through the catalyst bed inside the catalytic partial oxidizer (CPOX) where CH_4 reacts with oxygen to produce H_2. There are two main chemical reactions taking place in the CPOX: partial oxidation (POX) and total oxidation (TOX) [6, 7]:

$$(POX) \qquad CH_4 + \tfrac{1}{2}O_2 \rightarrow CO + 2H_2$$
$$\Delta H^0_{pox} = -0.036 \times 10^6 \text{ J/mol} \qquad (3)$$

$$(TOX) \qquad CH_4 + 2O_2 \rightarrow CO_2 + 2H_2O$$
$$\Delta H^0_{tox} = -0.8026 \times 10^6 \text{ J/mol}. \qquad (4)$$

Heat is released from both reactions. However, the TOX reaction releases more heat than the POX reaction. Hydrogen is created only in POX reaction and, therefore, it is preferable to promote this reaction in the CPOX. However, carbon monoxide (CO) is also created along with H_2 in the POX reaction as can be seen in (3). Since CO, even at concentrations of 10ppm [8], poisons the PEM fuel cell catalyst, it has to be eliminated using both the water gas shift converter (WGS) and the preferential oxidizer (PROX). In the WGS, water is injected into the gas flow in order to promote a water gas shift reaction:

$$(WGS) \qquad CO + H_2O \rightarrow CO_2 + H_2. \qquad (5)$$
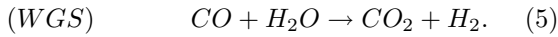
Note that even though the objective of WGS is to eliminate CO, hydrogen is also created from the WGS reaction. Oxygen is then injected (in the form of air) into the PROX reactor to convert the remaining CO:

$$(PROX) \qquad 2CO + O_2 \rightarrow 2CO_2. \qquad (6)$$
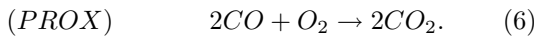
The hydrogen-rich mixture leaving the PROX enters the anode of the fuel cell stack where the electrochemical reaction takes place to convert H_2 to electrical power. The flow from the anode is then supplied to the CB where the excessive H_2 is burnt using the air supplied through a blower.

Finally, the flow from the CB is passed through two separate heat exchangers (HEX): one to preheat the air and one to pre-heat the fuel before they enter the FPS. This step is necessary to achieve the desired CPOX efficiency. High pre-heating temperatures lead to high CPOX efficiency. Taking into account the interconnection of the components, it can be concluded qualitatively that a large decrease in the CB temperature will reduce H_2 production and vise versa. Therefore, the maximum overall efficiency can not be achieved by component-level optimization. For example maximizing the FC efficiency does not effect linearly the overall efficiency [9, 10]. Instead, integration and coordination of the coupled system are essential for a highly effective CHP.

4 Control-Oriented CHP Model

The CHP model is developed with a focus on the dynamic behavior associated with the flows and pressures in the CHP, the temperature of the CPOX and the CB and the H_2 flow dynamics in particular.

4.1 Modeling Assumptions

Several assumptions are made in order to simplify the CHP model. Since the control of CO is not the subject of our investigation in this paper, the two reactors responsible for CO removal are lumped together as one volume and the combined volume is called WROX (WGS+PROX). The de-sulfurization process in the HDS is neglected by assuming pure CH_4 gas rather than natural gas. The HDS dynamics taken into account are the pressure and temperature dynamics. It is assumed that the air is 30% humidified and its composition entering the blower is constant . Finally, all gases obey the ideal gas law and all gas mixtures are perfect mixtures with homogenous composition that allows the application of lumped parameter models.

The modeling of the orifices, the blower, the mixer, the Hydro-Desulfurizer, the Water Gas Shift Converter and the Preferential Oxidation Reactor can be found in [2]. The components that are closely related to the CB recirculation loop are presented in the subsequent sections.

The states of the dynamic model are shown in Fig. 3. Where P stands for pressure, T, for temperature, subscripts, if any, denote the gas constituents and upperscripts identify the physical components.

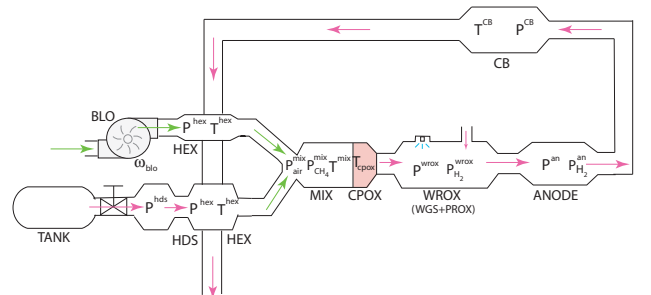Fig. 3: CHP model states

4.2 Catalytic Burner (CB)

In the catalytic burner the dynamics of the pressure and the temperature are taken into account. The mass balance equation and the ideal gas law for the CB yield

$$\frac{dm_{cb}}{dt} = (W^{cb}_{in} - W^{cb}_{out}), \qquad (7)$$

$$P_{cb}V_{cb} = \frac{m_{cb}}{M^{in}_{cb}}RT_{cb}, \qquad (8)$$

where $W_{in}^{cb} = W_{in}^{anode} + W_{in}^{air}$, and M_{cb}^{in} is the molecular weight of the incoming flow from the anode to the CB and is assumed to be constant. Also, since the H_2 concentration is only about 2-5% of the total flow, the difference between the H_2 mass reacted and the mass produced is neglected.

The pressure dynamics for the burner are modeled using the energy balance

$$m_{cb}c_P^{cb}\frac{dT_{cb}}{dt} = W_{in}^{cb}c_P^{in}(T_{in}^{cb} - T_{ref}) - \\ -W_{out}^{cb}c_P^{out}(T_{out}^{cb} - T_{ref}) - Q_r. \quad (9)$$

The heat release rate Q_r from burning the H_2 in the CB is modeled with

$$Q_r = \frac{Q_{LHV}^{H_2}}{M_{H_2}} \cdot min\left\{W_{H_2}, \frac{W_{in}^{air}}{\lambda}\right\} \quad (10)$$

where $\lambda = 34.2$ is the air to H_2 stoichiometry required in order for the total amount of H_2 to react

4.3   Heat Exchangers (HEX)

The dynamics considered in the heat exchangers for the air and the fuel include both pressure and temperature dynamics on the hot and the cold side. Using the mass balance principle and the ideal gas law, the pressure dynamics in each side of the heat exchanger are described by

$$\frac{dm_{hex}}{dt} = (W_{in}^{hex} - W_{out}^{hex}), \quad (11)$$

$$P_{hex}V_{hex} = \frac{m_{hex}}{M_{hex}^{in}}RT_{hex}, \quad (12)$$

where M_{hex}^{in} is the molecular weight of the incoming flow to the heat exchanger and is assumed to be constant. M_{hex}^{in}, in the case of the fuel heat exchanger, is the flow from the CB which is then passed to the air heat exchanger.

The internal energy balance yields the output temperatures in each side of the heat exchangers and is described by

$$\frac{dU_{hex}}{dt} = W_{hex}^{in}c_V^{in}(T_{hex}^{in} - T_{ref}) - \\ -W_{hex}^{out}c_V^{out}(T_{hex}^{out} - T_{ref}) \pm UA \cdot LMTD \quad (13)$$

where $T_{ref} = 273K$ is the reference temperature, UA is the heat transfer rate through the area of the HEX and LMTD is the logarithmic mean temperature difference between the hot and the cold side which, for a parallel co-flow heat exchanger arrangement, is defined as

$$(LMTD) = \frac{(T_{hot}^{in} - T_{cold}^{in}) + (T_{hot}^{out} - T_{cold}^{out})}{ln\frac{(T_{hot}^{in} - T_{cold}^{in})}{(T_{hot}^{out} - T_{cold}^{out})}}. \quad (14)$$

Finally the flow from the CB after it passes through the hot side of the fuel and air heat exchangers is released to the environment through the exhaust.

4.4 Catalytic Partial Oxidation (CPOX)

Pressure, temperature and composition dynamics are taken into account in the mixer, which is assumed to be in the same volume as the CPOX. In the CPOX, the energy balance is used to calculate the catalyst temperature, T_{cpx}:

$$m_{bed}^{cpx}C_{P,bed}^{cpx}\frac{dT_{cpx}}{dt} = \begin{bmatrix} \text{inlet} \\ \text{enthalpy} \\ \text{flow} \end{bmatrix} - \begin{bmatrix} \text{outlet} \\ \text{enthalpy} \\ \text{flow} \end{bmatrix} + \begin{bmatrix} \text{heat} \\ \text{from} \\ \text{reaction} \end{bmatrix}, \quad (15)$$

where m_{bed}^{cpx} (kg) and $C_{P,bed}^{cpx}$ (J/kg·K) are mass and specific heat capacity of the catalyst bed, respectively. The last two terms on the right hand side of (15) depend on the reaction taking place in the CPOX.
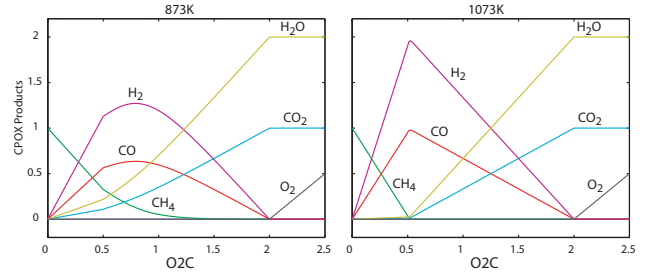

Fig. 4: CPOX products

In the catalytic partial oxidation reactor, methane (CH_4) is oxidized to produce hydrogen. Besides the POX and TOX reactions described in Section 3, the other two secondary reactions considered here are water formation, or hydrogen oxidation ($2H_2 + O_2 \rightarrow 2H_2O$), and carbon monoxide oxidation ($2CO + O_2 \rightarrow 2CO_2$). The species entering the CPOX include CH_4, O_2, H_2O, and N_2. The water may react with CH_4 through steam reforming reaction [5]; however, this reaction is ignored in this study. Methane reacts with oxygen to create the final product, which contains H_2, H_2O, CO, CO_2, CH_4, and O_2 [7]. The amount of each species depends on the initial oxygen to carbon (O_2 to CH_4) ratio, λ_{O2C}, of the reactants and the temperature of the CPOX catalyst bed, T_{cpx} as shown in Fig. 4. A set of equations is developed to calculate the conversion of the gases in CPOX. They are based on the reactions (3) and (4) and the thermodynamic equilibrium analysis in [7].

4.5   Anode (AN)

Mass conservation is used to model the pressure dynamics in the anode volume. The flows considered include flows into and out of the anode volume and the rate of hydrogen consumed in the fuel cell reaction. The dynamic equations are

$$\frac{dp^{an}}{dt} = \frac{RT_{an}}{M_{an}V_{an}}\left(W^{wrox} - W^{an} - W_{H_2}^{react}\right)$$

$$\frac{dp_{H_2}^{an}}{dt} = \frac{RT_{an}}{M_{H_2}V_{an}}\left(x_{H_2}^{wrox}W^{wrox} - x_{H_2}^{an}W^{an} - W_{H_2}^{react}\right)$$

where W^{an} is calculated as a function of the anode pressure, p^{an}, and the ambient pressure, p_{amb}. The

rate of hydrogen reacted is a function of stack current, I_{st}, through the electrochemistry principle [11]

$$W_{H_2}^{react} = M_{H_2} \frac{nI_{st}}{2F} \qquad (16)$$

where n is the number of fuel cells in the stack and F is the Faraday's number (96485 coulombs).

Two variables used to monitor the performance of the system are hydrogen utilization, U_{H_2}, and anode hydrogen mole fraction, y_{H_2}, used to monitor anode starvation conditions . They can be calculated by

$$U_{H_2} = \frac{H_2 \text{ reacted}}{H_2 \text{ supplied}} = \frac{W_{H_2}^{react}}{x_{H_2}^{wrox} W^{wrox}} \qquad (17)$$

$$y_{H_2} = \frac{p_{H_2}^{an}}{p^{an}}. \qquad (18)$$

5 Performance analysis

In this section, we present initial results on system dynamics based on the model developed in Section 4. The air and the fuel are controlled by a simple feed-forward control scheme. In particular, we focus on the different responses of the system with and without the CB. Figures 5, 6 and 7 illustrate the response of the systems to different current step commands.
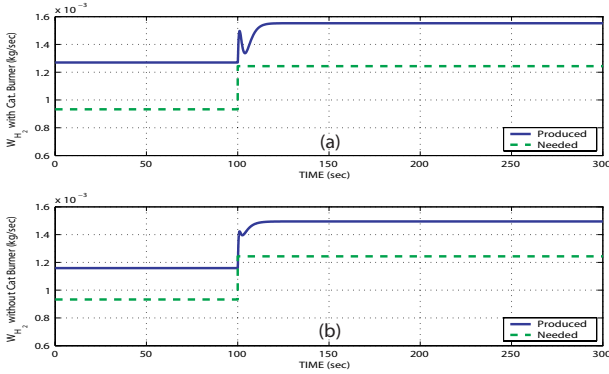

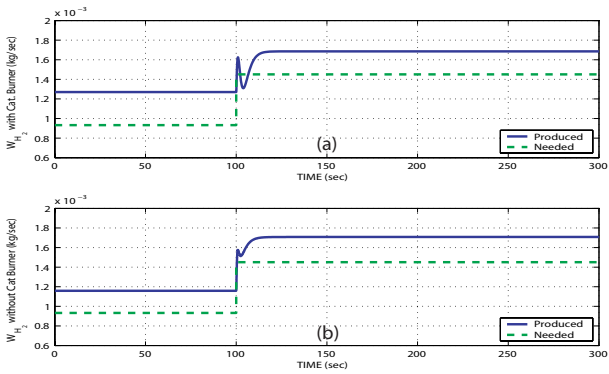Fig. 5: H_2 generation during a 90-110A step, with (a) and without (b) the CB

Fig. 6: H_2 generation during a 90-150A step, with (a) and without (b) the CB

For a small load step (90-110A), both the system with and without the CB generate enough H_2 so as not to starve the anode (Fig. 5). A larger load step
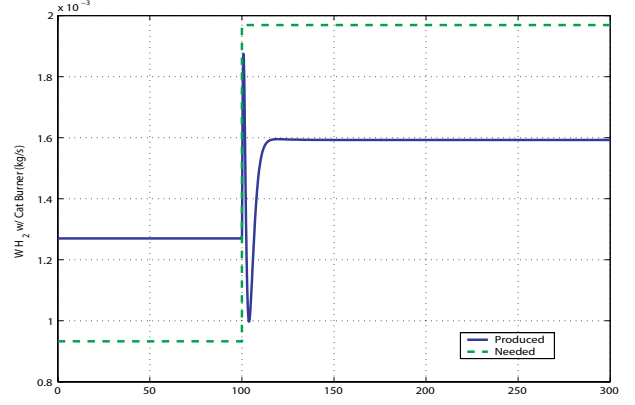

Fig. 7: H_2 generation during a 90-190A step with CB

command (90-150A) depletes the H_2 from the anode and causes the system with the CB to produce less H_2 than that required for a short period of time (Fig. 6). However, the system recovers and the desired steady state performance is sustained. If an even larger load is applied (90-190A), then the long H_2 starvation will lead to a system light off or more probable in damaging the anode (Fig. 7). Generating less amount of H_2 than that required by the load command, besides starving the anode, results in a substantial temperature drop in the CB. Consequently the fuel and air temperatures entering the CPOX to drop which in turn causes the H_2 generation to drop as well. This will lead to failure of the PEM-FC, unless the load is removed.

The performance of the CHP system with a CB can be explained by examining the CPOX temperature (T_{cpx}). As seen in Fig. 4, the CPOX products are a function of the T_{cpx} and the oxygen to carbon ratio. The T_{cpx} is a function of the temperature of the inlet flow and the temperature produced from the reactions that take place inside the CPOX - mainly by the TOX reaction (4) since it is highly exothermic compared to the POX (3). To optimize the reforming efficiency given that the TOC reaction does not contribute to the H_2 generation, the temperature in the CPOX has to be provided mainly by the preheated inlet flow and not by the TOX reaction, while the oxygen to carbon ratio is around 0.5-0.6.

When external heating of the inlet flow is employed, one can assume nearly perfect regulation of the inlet
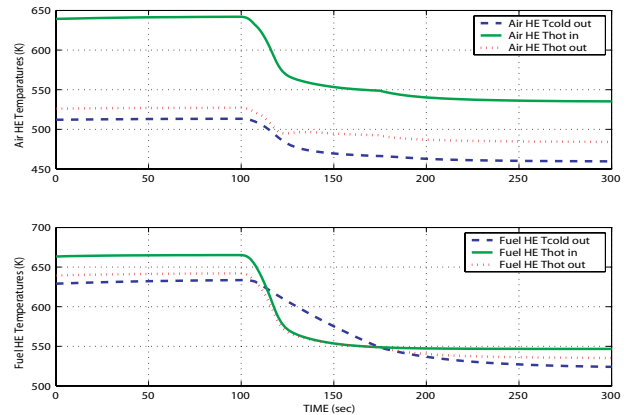

Fig. 8: Heat Exchanger flow temperatures for a 90-150A step with a CB

flow temperature, independently of step changes in the fuel cell load demand. Fast H_2 generation relies then in accurate control of the O2C ratio in the mixer by coordinated regulation of the air and the fuel flow [12]. The control difficulty in this scheme increases when utilization increases.

In the case of the CHP system, slightly lower utilization is allowed because the excess H_2 is used to heat the FPS inlet flow. However the inlet flow temperature drops significantly during a transient because of H_2 flow decrease to the CB. For the step 90-190A the inlet flow temperature profiles are shown in Fig. 8. The temperature drop shown in Fig. 8 and its effects to the CPOX products shown by (Fig. 4), clarify that the poor transient behavior of the CHP system is caused due to the interaction between the power and thermal loops.

6 Transient Response Improvement of the CHP System

There are several control options to prevent the H_2 starvation in both CB and the stack. One is to maintain a constant CB temperature by controlling the air to the burner while always providing excess H_2. This option will result in an oversized CB and aggravate the potential CB melt-down problem during load step-down. Another option is to schedule air and methane flow to higher steady state oxygen to carbon stoichiometry operating point so that TOC reaction will be enhanced to provide more heat to the CPOX. Both options will result in lower H_2 utilization in the fuel cell stack or lower H_2 production in the CPOX thus a lower overall efficiency. The second option, however, can be dynamically scheduled to affect minimally the overall system efficiency and only take effect during a transient.
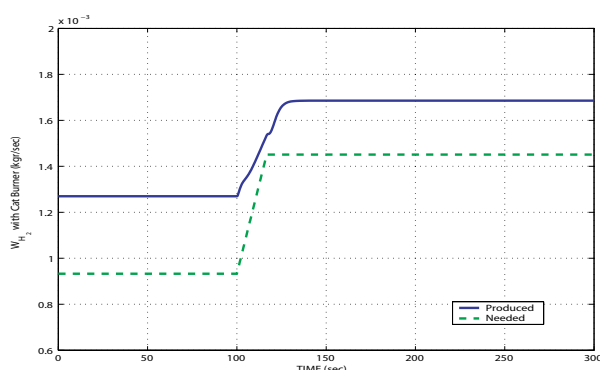

Fig. 9: H_2 generation during a 90-150A step when using a rate limiter

Another interesting and efficient method of protecting the system during a transient is the use of a rate limiter so that the fuel processor has enough time to ramp-up its H_2 production levels. The result for a load step from 90-150A with a rate limiter of 4A/sec is shown in Fig. 9. Compared to the plot shown in Fig. 6, the system can maintain the H_2 generation above the desired value all the time.

However, in the case of a larger step command, a rate limiter would cause a very large time delay thus a more elaborated feedback control scheme is required. A reference governor like the one developed for the dual problem of oxygen starvation in [13], combined with an adaptive setpoint schedule of O2C ratio, will be pursued next.

7 Conclusions

A dynamical model of an integrated fuel cell stack, fuel processor and catalytic burner is developed. The efficiency improvement and the performance of the CHP system are the main issues analyzed in this paper. A solution for preventing H_2 starvation in fuel cell and catalytic burner during load transients is proposed as well, which includes a reference governor combined with a supervisory controller for O2C setpoint adaptation. Incorporating this control scheme is the next step of this project, which is made possible by the dynamic model described herein.

References

[1] A.L. Dicks. Hydrogen generation from natural gas for the fuel cell systems of tomorrow. *Journal of Power Sources*, 61:113–124, 1996.

[2] J.T. Pukrushpan, A.G. Stefanopoulou, and S. Varigonda. Control-oriented model of fuel processor for hydrogen generation in fuel cell applications. *IFAC Symposium on Advances in Automotive Control*, April 2004.

[3] E.D. Doss, R. Kumar, R.K. Ahluwalia, and M. Krumpelt. Fuel processors for automotive fuel cell systems: a parametric analysis. *Journal of Power Sources*, 102:1–15, 2001.

[4] T.H. Gardner, D.A. Berry, K.D. Lyons, S.K. Beer, and A.D. Freed. Fuel processor integrated H_2S catalytic partial oxidation technology for sulfur removal in fuel cell power plants. *Fuel*, 81:2157–2166, 2002.

[5] L.F. Brown. A comparative study of fuels for on-board hydrogen production for fuel-cell-powered automobiles. *International Journal of Hydrogen Energy*, 26:381–397, 2001.

[6] A.L. Larentis, N.S. de Resende, V.M.M. Salim, and J.C. Pinto. Modeling and optimization of the combined carbon dioxide reforming and partial oxidation of natural gas. *Applied Catalysis*, 215:211–224, 2001.

[7] J. Zhu, D. Zhang, and K.D. King. Reforming of CH_4 by partial oxidation: thermodynamic and kinetic analyses. *Fuel*, 80:899–905, 2001.

[8] John W. Weidner Andrew T. Haug, Ralph E. White. Development of a novel co tolerant proton exchange membrane fuel cell anode. *Journal of The Electrochemical Society*, 149 (7), 2002.

[9] Christos A. Frangopoulos Nectarios C. Monanteras. Towards synthesis optimization of a fuel-cell based plant. *Energy Conversion & Management*, 40, 1999.

[10] Whitney G. Colella. Design considerations for effective control of an afterburner sub-systemin a combined heat and power (chp) fuel cell system (fcs). *Journal of Power Sources*, 118, 2003.

[11] James Larminie and Andrew Dicks. *Fuel Cell Systems Explained*. John Wiley & Sons Inc, West Sussex, England, 2000.

[12] J.T. Pukrushpan, A.G. Stefanopoulou, S. Varigonda, L.M. Pedersen, S. Ghosh, and H. Peng. Control of natural gas catalytic partial oxidation for hydrogen generation in fuel cell applications. *Proceedings of the 2003 American Control Conference*, pages 2030–2036, 2003.

[13] Jing Sun and Ilya Kolmanovsky. A robust load governor for fuel cell oxygen starvation protection. *Proceedings of 2004 American Control Conference*, June 2004.